

AD _____

Award Number: DAMD17-99-1-9056

TITLE: Isolation of Motile Tumor Cells from Live Breast Tumors

PRINCIPAL INVESTIGATOR: John Condeelis, Ph.D.

CONTRACTING ORGANIZATION: Albert Einstein College of Medicine
Bronx, New York 10461

REPORT DATE: June 2000

TYPE OF REPORT: Annual

PREPARED FOR: U.S. Army Medical Research and Materiel Command
Fort Detrick, Maryland 21702-5012

DISTRIBUTION STATEMENT: Approved for Public Release;
Distribution Unlimited

The views, opinions and/or findings contained in this report are those of the author(s) and should not be construed as an official Department of the Army position, policy or decision unless so designated by other documentation.

REPORT DOCUMENTATION PAGE

Form Approved
OMB No. 074-0188

Public reporting burden for this collection of information is estimated to average 1 hour per response, including the time for reviewing instructions, searching existing data sources, gathering and maintaining the data needed, and completing and reviewing this collection of information. Send comments regarding this burden estimate or any other aspect of this collection of information, including suggestions for reducing this burden to Washington Headquarters Services, Directorate for Information Operations and Reports, 1215 Jefferson Davis Highway, Suite 1204, Arlington, VA 22202-4302, and to the Office of Management and Budget, Paperwork Reduction Project (0704-0188), Washington, DC 20503

1. AGENCY USE ONLY (Leave blank)		2. REPORT DATE June 2000	3. REPORT TYPE AND DATES COVERED Annual (1 Jun 99 - 31 May 00)	
4. TITLE AND SUBTITLE Isolation of Motile Tumor Cells from Live Breast Tumors			5. FUNDING NUMBERS DAMD17-99-1-9056	
6. AUTHOR(S) John Condeelis, Ph.D.				
7. PERFORMING ORGANIZATION NAME(S) AND ADDRESS(ES) Albert Einstein College of Medicine Bronx, New York 10461 E-MAIL: condeeli@aecom.yu.edu			8. PERFORMING ORGANIZATION REPORT NUMBER	
9. SPONSORING / MONITORING AGENCY NAME(S) AND ADDRESS(ES) U.S. Army Medical Research and Materiel Command Fort Detrick, Maryland 21702-5012			10. SPONSORING / MONITORING AGENCY REPORT NUMBER	
11. SUPPLEMENTARY NOTES This report contains colored photos				
12a. DISTRIBUTION / AVAILABILITY STATEMENT Approved for public release; distribution unlimited			12b. DISTRIBUTION CODE	
13. ABSTRACT (Maximum 200 Words) During metastasis from a primary tumor, cell motility is believed to be important for dissemination of tumor cells from the primary. An understanding of the mechanisms of cell motility in metastatic tumor cells <i>in vivo</i> , in particular, would be important for a more rational system of diagnosis and treatment of metastatic cancers. We have developed a new method for imaging tumor cells in live animals and have identified subpopulations of moving cells within primary breast tumors. Previous to this approved application, we described only a metastatic cell-line (MTLn3) using this technique. Since then, we have described a non-metastatic cell line (MTC) and reported the observable differences between the two cell lines. We proposed to use this novel imaging method to collect the motile subpopulation of tumor cells in live primary tumors which can then be used for further analysis to define how these cells differ from their non-motile neighbors in the same tumor and to define how cell motility contributes to metastasis. We have been able to differentially collect the motile sub-population of metastatic cells and shown that due to the differing chemotactic response to EGF, we were able to selectively collected the metastatic cell				
14. SUBJECT TERMS Breast Cancer		20010302 070		15. NUMBER OF PAGES 38
				16. PRICE CODE
17. SECURITY CLASSIFICATION OF REPORT Unclassified	18. SECURITY CLASSIFICATION OF THIS PAGE Unclassified	19. SECURITY CLASSIFICATION OF ABSTRACT Unclassified	20. LIMITATION OF ABSTRACT Unlimited	

FOREWORD

Opinions, interpretations, conclusions and recommendations are those of the author and are not necessarily endorsed by the U.S. Army.

___ Where copyrighted material is quoted, permission has been obtained to use such material.

___ Where material from documents designated for limited distribution is quoted, permission has been obtained to use the material.

___ Citations of commercial organizations and trade names in this report do not constitute an official Department of Army endorsement or approval of the products or services of these organizations.

X In conducting research using animals, the investigator(s) adhered to the "Guide for the Care and Use of Laboratory Animals," prepared by the Committee on Care and use of Laboratory Animals of the Institute of Laboratory Resources, national Research Council (NIH Publication No. 86-23, Revised 1985).

N/A For the protection of human subjects, the investigator(s) adhered to policies of applicable Federal Law 45 CFR 46.

N/A In conducting research utilizing recombinant DNA technology, the investigator(s) adhered to current guidelines promulgated by the National Institutes of Health.

N/A In the conduct of research utilizing recombinant DNA, the investigator(s) adhered to the NIH Guidelines for Research Involving Recombinant DNA Molecules.

N/A In the conduct of research involving hazardous organisms, the investigator(s) adhered to the CDC-NIH Guide for Biosafety in Microbiological and Biomedical Laboratories.

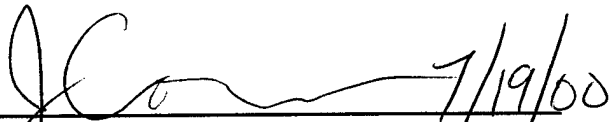

PI - Signature 7/19/00
Date

Table of Contents

Cover.....	1
SF 298.....	2
Foreword.....	3
Table of Contents.....	4
Introduction.....	5
Body.....	6-8
Key Research Accomplishments.....	8
Reportable Outcomes.....	8
Conclusions.....	9
References.....	10
Appendices.....	10

Introduction

We have developed a model that directly examines the motility of non-metastatic and metastatic tumor cells in live primary tumors *in situ*. Through the use of this model we have observed the locomotion of metastatic cells and cell surface features of these movements in live animals. It is clear that metastatic tumor cells are actively motile as they disseminate from the primary site. This information supports the three-step hypothesis of metastasis which proposes that motility is necessary for a cell to metastasize. This model will be useful in describing and tracking the behavior and interactions of these metastatic tumor cells *in vivo*. In addition, it represents an opportunity to reliably procure pure populations of motile tumor cells *in vivo* under direct observation.

Our specific aims are to collect pure populations of motile tumor cells by chemotaxis of tumor cells to EGF and serum into a catheter and, alternatively, collect motile tumor cells by laser capture microdissection from tissue sections of a marked population of cells that had been documented previously to be motile using intravital imaging.

These cells can be used as a micro biopsy to examine gene expression patterns unique to the motile and potentially metastatic population of cells in the primary tumor. This sub-population can be compared with adjacent but distinct populations of cells in the same tissue field by using laser capture micro-dissection. Both methods of procurement of pure cell populations will allow quantitative analyses using methods based on polymerase chain reaction, reverse transcriptase PCR, chromosome mapping and conventional immuno assay. This will define for the first time how these motile cells differ from their non-motile neighbors in the same tumor and from cells in non-metastatic tumors at the level of gene and protein composition and expression. Such analyses will lead to the discovery of genes associated with the motile phenotype in invasive and metastatic tumors which may have diagnostic and prognostic value.

Technical Objectives

To achieve the goal of collecting pure subpopulations of motile cells from live primary tumors, we proposed two approaches:

1. Collection into a catheter of a population of cells documented to be motile by intravital imaging.
2. Collection by Laser Capture Microdissection of a marked population of cells documented to be motile by intravital imaging.

The following is a brief description of our research accomplishments. A complete description can be found in the manuscripts included in the appendices.

To test the ability to collect motile chemotactic cells into a microneedle using matrigel as a substrate, we first performed the experiment *in vitro* with cultured metastatic adenocarcinoma cells (MTLn3) against a range of EGF concentrations from 0.5 nM to 250 nM EGF (1; included in appendices). After collecting the cells for up to 6 h, we found an 8-fold increase of cells collected over needles with buffer alone at a concentration of 25 nM EGF. With a needle containing matrigel mixed 1:1 with 25 nM EGF, we were able to visualize the MTLn3 cells orienting toward and moving in the direction of the matrigel substrate (1).

After further characterization of the tumors generated by the metastatic MTLn3 cells and the non-metastatic MTC cells using the intravital imaging system we developed, we were able to find distinct differences between the two tumors (2; included in appendices). We found that the MTLn3 cells are only elongated and polarized when in association with blood vessels, while the MTC cells are elongated and polarized randomly throughout the tumor. While both cell types have the same approximate speed

and move in a persistent linear motion, MTLn3 cells only move when near or in contact with a surrounding vessel and there is a higher degree of host cell involvement in the metastatic tumor (2, 3). MTC cells move linearly throughout the tumor and are seen to fragment easily especially when invading a vessel. Also, cells can be collected from the right atrium of the heart of animals with MTLn3 tumors at a 90-fold greater efficiency than from animals with MTC tumors (2).

By performing the *in vivo* invasion assay using the microneedles, we were able to selectively collect the motile MTLn3 cells from the living tumor at a greater efficiency than the MTC cells (1). Using microneedles filled with matrigel mixed 1:1 with buffer, 25nM EGF or 10% serum, we were able to collect MTLn3 cells at a 10-fold greater rate than MTC cells in buffer alone. Directly comparing the two tumor types with needles under identical conditions, 15x more MTLn3 cells enter the microneedles containing EGF than MTC cells, and 6x more in the needles containing serum. There is a 2-fold increase of MTC cells entering the serum containing needle over buffer-alone. This is a significant increase over background and is confirmed by the fact that MTC cells show a similar protrusive response to serum *in vitro* as MTLn3 cells but to a lesser degree. MTLn3 cells enter the buffer-alone needle 4x more than the MTC cells under similar conditions. This is possibly due to the chemoattractants found in the matrigel or to the ability of the MTLn3 cells to create a chemotactic gradient by proteolyzing the matrigel into small chemoattractant peptides (1).

The use of laser capture microdissection (LCM) has not been developed because the necessary equipment has not arrived at this point during the course of the funding. In

addition, the collection of the motile cells from the primary tumor was successful and specific enough to allow for further experiments and interpretations, without the need for LCM.

Key Research Accomplishments

3. Characterization of non-metastatic cells in an *in vivo* primary tumor by intravital imaging.
4. The analysis of intravasation at the primary tumor and the differences between metastatic and non-metastatic cells *in vivo*.
5. The collection of the motile population of cells from a primary using a catheter filled with a chemoattractant mixed 1:1 with matrigel.

Reportable Outcomes

Wyckoff, J., Segall, J.E., and Condeelis, J. (2000) The collection of the motile population of cells from a living tumor. (submitted)

Wyckoff, J., Jones, J., Condeelis, J., and Segall, J. (2000) A Critical Step in Metastasis: *In vivo* Analysis of Intravasation at the Primary Tumor. *Cancer Research* 60:2504-2511

Condeelis, J., Jones, J., Wyckoff, J., and Segall, J. (2000) Imaging of primary tumors in whole animals using laser-based tomography. Abstract and presentation, American Assoc. of Cancer Research.

Segall, J., Wyckoff, J., Bailly, M., Jones, J., and Condeelis, J. (2000) The rate-limiting step in metastasis: *in vivo* analysis of intravasation at the primary tumor. Abstract and presentation, American Assoc. of Cancer Research.

Funding:

Data collected as a result of this USAMRMC grant has been used in a PAR-99-100, R21/R33 NIH grant application entitled "Innovative Technologies for the Molecular Analysis of Cancer: Phased Innovation."

Conclusions

Since motility plays an important role to the dissemination of tumor cells, the need to understand the mechanistic and physical elements that allow cells to intravasate or extravasate needs to be studied at the molecular and protein level. Hence, there is a need to be able to differentially separate the motile subpopulation of cells from the nonmotile and host tissue that surrounds it. By taking advantage of the inherent chemotactic motility of a metastatic cell, we were able selectively collect the cells within the primary tumor that have the ability to leave the tumor. These cells then can be compared to cells taken from the primary tumor, from the blood and from metastases and by proteomic and genomic assays, differences between these cells can be discovered at the molecular level. Since metastasis is the major cause of mortality in breast cancer patients, discovering how the cells have the ability to metastasize can lead to treatment and prevention. Developing ways to stop motility at the molecular level can in the future lead to means of preventing metastasis. Our ability to collect the motile subpopulation and at the same time image the primary tumor, so as to differentiate between metastatic and nonmetastatic tumors and cells, will allow for both the ability to discover these molecular differences and to test possible preventive treatments in the fight against breast cancer and metastatic cancers in general.

References

Wyckoff, J., Segall, J.E., and Condeelis, J. (2000) The collection of the motile population of cells from a living tumor. (submitted)

Wyckoff, J., Jones, J., Condeelis, J., and Segall, J. (2000) A Critical Step in Metastasis: *In vivo* Analysis of Intravasation at the Primary Tumor. *Cancer Research* 60:2504-2511

Farina, K.L., Wyckoff, J.B., Rivera, J., Lee, H., Segall, J.E., Condeelis, J.S., Jones, J.G. (1998) Cell motility of tumor cells visualized in living intact primary tumors using green fluorescent protein. *Cancer Research* 58:2528-2532.

Appendices

Included:

Wyckoff, J., Segall, J.E., and Condeelis, J. (2000) The collection of the motile population of cells from a living tumor. (submitted)

Wyckoff, J., Jones, J., Condeelis, J., and Segall, J. (2000) A Critical Step in Metastasis: *In vivo* Analysis of Intravasation at the Primary Tumor. *Cancer Research* 60:2504-2511

Condeelis, J., Jones, J., Wyckoff, J., and Segall, J. (2000) Imaging of primary tumors in whole animals using laser-based tomography. Abstract and presentation, American Assoc. of Cancer Research.

Segall, J., Wyckoff, J., Bailly, M., Jones, J., and Condeelis, J. (2000) The rate-limiting step in metastasis: *in vivo* analysis of intravasation at the primary tumor. Abstract and presentation, American Assoc. of Cancer Research.

**The collection of the motile population of cells from a living
tumor**

Jeffrey B. Wyckoff^{*}, Jeffrey E. Segall^{*}, and John S. Condeelis^{*†}

**Departments of Anatomy and Structural Biology^{*}
Albert Einstein College of Medicine
1300 Morris Park Avenue
Bronx, NY 10461**

†Corresponding author

Telephone: 718-430-4068

FAX: 718-430-8996

Email: condeeli@aecom.yu.edu

Running title:

Key words: invasion, metastasis, cell motility, matrigel

Abstract

In this study we report that needles containing chemoattractants can be used to collect the subpopulation of motile and chemotactic tumor cells from a primary tumor in a live rat as a pure population suitable for further analysis. The most efficient cell collection requires the presence of chemotactic cytokines such as EGF and serum components and occurs with 15 fold higher efficiency in metastatic tumors compared to non-metastatic tumors. Even though tumor cells of the non-metastatic tumors show a motility response to serum, they were not collected with high efficiency into needles *in vivo* in response to serum indicating that additional factors besides motility are required to explain differences in cell collection efficiencies between metastatic and non-metastatic tumors. The results reported here indicate that needles filled with growth factors and matrigel, when inserted into the primary tumor, can faithfully mimic the environment that supports invasion and intravasation *in vivo*. Furthermore, the results indicate that the same cell behaviors that contribute to chemotaxis *in vitro* also contribute to invasion *in vivo*.

INTRODUCTION

Metastasis involves the escape of cells from the primary tumor either via lymphatics or blood vessels, transport to and arrest in a target organ, and growth of metastasis in the target organ (1). Each of these steps is a multicomponent process, with potentially different tumor cell properties and molecules playing critical roles at different steps (2). Recently, emphasis has been on the development of molecular arrays to identify new genes and proteins that contribute to specific steps in metastasis. Such approaches are crucial in the analysis of cancer as a genetic disease and in the identification of key genes that might be used in diagnosis and therapy. However, array-based approaches treat the tumor as a black box. Ideally, high resolution methods for the analysis of metastasis at the cellular level, such as imaging of cells within tumors, when combined with array based approaches, could be used to accurately evaluate the roles of specific gene products in the individual steps of metastasis at the cellular level. The use of Laser Capture Microdissection as a front end for array-based gene discovery is such a fusion approach (3). However, some of the cell behaviors that are believed to be essential for metastasis such as adhesion and motility (4,5) cannot be used as criteria in the selection of cells for analysis from fixed material because the behavior and history of individual cells cannot be inferred from fixed material. Methods for the collection of cells from living tumors in which key cell behaviors can be observed and used as the criteria for cell collection, need to be developed. One such cell behavior is the chemotaxis of tumor cells. Metastatic tumor cells are believed to chemotax to cytokines that are normally found in association with blood vessels (6, 7, 11). We developed a cell graft breast tumor metastasis model in rats that is syngeneic and orthotopic that permits

the imaging and tracking of cell behavior in live tumors (8, 11). Using this model, we have observed, in metastatic primary tumors, the highly persistent linear locomotion of a subpopulation of tumor cells toward blood vessels *in vivo* using intravital imaging. This locomotion resembles the chemotaxis of cells observed in culture (8, 9) and is correlated with metastatic potential (9, 10). Tumor cell chemotaxis is also correlated with the accumulation of metastatic tumor cells around, and their polarization toward, blood vessels in the primary tumor. Furthermore, chemotaxis is correlated with the efficient intravasation into, and survival of tumor cells in, the systemic circulation (11). Since these properties are not observed in non-metastatic tumors prepared from cells in the same way (7, 11), polarization and chemotaxis toward blood vessels are believed to be important in intravasation and metastasis (11). In this study we report that chemotaxis can be used to advantage to collect the subpopulation of motile and chemotactic tumor cells from a primary tumor *in vivo* as a pure population suitable for further analysis.

Materials and Methods:

Serum upshift of cells *in vitro*

MTLn3-GFP and MTC-GFP cells were plated in 35mm dishes at a density of 50,000 cells per dish 18 h prior to the experiment. On the day of the experiment, cells were starved for 3 h in 2 mls of MEM containing HEPES and 0.69% BSA, which is the isotonic equivalent of 10% FBS. The upshift was performed as described before (12), with the exception that the cells were stimulated with 10% FBS. Briefly, the dishes were covered with a thin layer of heavy mineral oil (Sigma # 400-5) and placed in an enclosed microscope pre-heated to 37° c. Using a CCD camera, single frame images were

collected using NIH Image every minute. After 4 minutes, 2 ml of MEM with HEPES and 20% FBS were added to the dish and image frames were collected for 16 more minutes.

***In vitro* cell collection**

MTLn3 cells were plated in a 35 mm dish 18 h prior to the experiment so as to be 60-80 % confluent at the time of the experiment. On the day of the experiment, cells were starved using MEM with 0.35% BSA (MEM-BSA), the isotonic equivalent of 5% FBS, for 2 h. During this time, 26-gauge syringe needles were prepared by filling them with 10 ul of Matrigel mixed 1:1 with MEM-BSA or MEM-BSA containing EGF for a final concentration of 0.5nM, 2.5nM, 5nM, 25nM, 50nM, or 250nM EGF. After starvation the needles were attached to the side of the plate using paraffin to hold them in place with the bevel of the needle facing the bottom of the plate so that the matrigel was in contact with the surface of the plate. Dishes were placed into a 37° c / 5.0% CO₂ incubator for up to 6 h. After this time, the contents of each needle was extruded into a new 35-mm dish containing MEM with 5% FBS (growth medium). Cells that had entered the needle were allowed to grow into clones for 6 days to determine cell count and viability. Positive clones, checked by GFP fluorescence and cell morphology, were then counted.

To image the cells moving toward the needle, a dish was plated for 40-50% confluency before the experiment. Cells were starved and a needle was prepared as above containing matrigel mixed 1:1 with MEM-BSA containing 25nM EGF. Images as single

frames were taken using the heated microscope and NIH Image every 30 min as described above. The dish was kept in a 37° c/ 5% CO2 incubator between images.

***In vivo* cell collection**

MTLn3-GFP and MTC-GFP cells were injected into female Fischer 344 rats as described before (8,11) and tumors were allowed to grow for 2.5 weeks. On the day of the experiment, 33-gauge needles were prepared as above by filling them with matrigel and MEM-BSA, MEM-BSA with a final EGF concentration of 25 nM, or MEM-BSA with a final FBS concentration of 10%. All needles included 0.01mM EDTA, pH 7.4 to sequester heavy metals that might be released by the needle. A rat was anesthetized using 5% isoflurane and laid on its back. The isoflurane was reduced to 2% and a small patch of skin over the tumor was removed. Three 25-gauge needles (guide needles) with blocking wires were inserted to a depth of 2 mm. The blocking wire was removed and one of the matrigel filled needles was inserted into each guide needle (as shown in Figure 3). The needle was then left in the tumor for 6 h. The isoflurane concentration was slowly lowered to 0.5% during the course of the experiment so as to keep the rat's breathing even and unlabored. After 6 h, the needles were withdrawn, extruded into 35mm dishes containing growth medium and all cells were counted immediately. The percent of cells with GFP fluorescence was determined.

As a control for the effects of matrigel, a 33-gauge needle was filled as above with MEM-BSA and agarose, for a final concentration of 1% and the *in vivo* experiment was performed as above.

Results

***In vitro* cell collection**

As has been shown previously, MTLn3 cells are chemotactic to EGF with an optimum concentration at 5 nM EGF (12). Also, it has been shown that MTLn3 cells, when placed in a gradient generated using a pipet filled with 50 μ M EGF, will orient toward and locomote in the direction of the pipet exhibiting true amoeboid chemotaxis (9). MTLn3 cells are metastatic when reinjected into the mammary fat pad of a Fischer 344 rat. We prepared an artificial microenvironment using microneedles filled with matrigel and either EGF or serum as the chemoattractant in order to simulate invasion and intravasation into a container that could be withdrawn to collect the chemotactic/invasive subpopulation of cells.

To establish the concentration necessary to attract MTLn3 cells into the needle, needles were filled with a range of EGF concentrations from 0.5 nM to 250 nM and inserted into a cell culture. At times up to 6 h of collection, the needles were withdrawn from the culture and the contents were extruded into a new dish with growth medium and the cells were allowed to grow for 6–7 days to determine cell counts and test viability. The number of cells entering the needle was determined by the number of GFP fluorescent clones that grew during this time. At the peak concentration of 25 nM EGF, an 8-fold increase in the number of cells entering the needle was seen, when compared to buffer alone (Figure 1). The number of cells collected decreased at 50 nM EGF, and by 250nM EGF, the number of cells collected returned to near background.

The differences in EGF concentration optimum for cell response between the upshift (5 nM, (12)), the pipet experiment (50 μ M, (9)) and the collection experiment reported here (25 nM) can be explained by the differences in diffusion of EGF in the different experimental designs. In the upshift, there is no gradient involved and the cells see an equal and constant concentration of EGF. For the pipet experiment the gradient is created by a pipet with an i.d. of $<1 \mu\text{m}$ and the concentration outside of the pipet is only a fraction of the concentration in the pipet. For the *in vitro* cell collection experiments reported here, the i.d. of a 26-gauge needle is 250 μm ; hence a larger % of EGF is delivered per unit time so that a much lower EGF concentration is necessary than in the pipet experiment (9).

By using a needle loaded with matrigel and 25 nM EGF in MEM-BSA, we were able to capture images of the cells moving toward the pipet, using time-lapse video-microscopy. In Figure 2, the matrigel surface at the edge of the needle is delineated by the white line and colored gray. At time zero, cells 1 and 2 are seen as non-polarized cells with no discernable leading edge. After 1.5 h, cells 1 and 2 have oriented themselves toward and moved in the direction of the needle induced EGF gradient, extending a leading lamellapod towards the needle. Cell 3 has also moved into the field. After 3 h, all three cells can be seen to have moved measurably closer to the needle. The cells move toward the needle at a velocity of 0.32 $\mu\text{m}/\text{min}$ which is comparable to the velocities reported previously (9).

***In vivo* Cell collection**

To determine if cells can be collected from tumors *in vivo*, and if so, if there is a difference in collection efficiency of cells from non-metastatic and metastatic tumors, experiments were performed by placing needles into the primary tumors generated by either the non-metastatic MTC-GFP or the metastatic MTLn3-GFP cell-lines. For this, a 33-gauge needle (i.d. = 125 μ m) was filled as above and inserted into the guide syringe after a blocking wire was removed (as modeled in Figure 3). The needles were filled with matrigel plus either buffer, 25nM EGF, or 10% FBS. The 10% FBS was used because the motility of both MTLn3 cells and MTC cells is stimulated in response to 10% serum (data not shown). After 6 h of collection, needles were withdrawn and the contents of each was extruded into a 35mm dish containing growth medium and collected tumor cells were determined by GFP fluorescence. To confirm that only GFP labeled cells were in the needle, 1 μ g/ml DAPI was added to the dish to stain all cells. All DAPI stained nuclei were in GFP labeled cells, indicating that only tumor cells were collected.

The number of cells collected for each condition was normalized to the number of cells collected from the MTC-GFP tumors using needles containing matrigel plus buffer (MEM-BSA) only (Figure 4). For the needle with 25nM EGF, 15.3-times more MTLn3 cells were collected from metastatic MTLn3 tumors compared to MTC cells from non-metastatic MTC tumors under the same conditions of collection. In this case a maximum of 100 cells was collected. Needles containing 10% FBS showed only a 6.0-fold difference between the two tumor types under the same conditions (Figure 4). There was a 2-fold increase in the number of MTC cells entering the 10% FBS needle from the MTC tumors compared to the number of cells that entered the needle containing only buffer. This difference was shown to be significant (t-test value = 0.027), and is

consistent with the increase in motility of MTC cells when stimulated with 10% FBS *in vitro* (data not shown).

In addition, in needles containing only buffer, 4.3-times more tumor cells were collected from MTLn3 tumors than from MTC tumors (Figure 4). To determine if this was due to a cell response to matrigel, a needle was filled with either 1% agarose containing MEM-BSA or 1% agarose containing 10% FBS in MEM-BSA. MTLn3 cells are able to adhere and grow on agarose. However, agarose was chosen because it is a polysaccharide that cannot be degraded by proteases. The number of cells entering the agarose needles was at background for both the 10% FBS containing needle (data not shown) and the needle with buffer alone (Figure 4) indicating that either components within the matrigel or the degradation of matrigel provides a chemotactic signal to the cells.

Discussion

In this study we report that needles containing chemoattractants can be used to collect the subpopulation of motile and chemotactic tumor cells from a primary tumor *in vivo* as a pure population suitable for further analysis. Our results demonstrate that tumor cells are collected into needles that have been inserted into a primary tumor when they contain either serum, EGF or matrigel but not agarose, indicating that a tactic signal is required for collection. The most dramatic accumulation of cells in the needles occurs in response to either EGF or serum. EGF is known to be a chemoattractant for MTLn3 cells (9) while serum stimulates the motility of both MTLn3 and MTC cells. However, matrigel was sufficient to collect cells above background indicating that either the matrigel

contains cytokines that are chemotactic for these cells or that limited proteolysis resulting from the interaction of the matrigel with the tumor is sufficient to generate a gradient of chemotactic peptides. Either possibility is consistent with the known properties of matrigel (17, 18). Furthermore, MTLn3 cells have a 4-fold greater collagenase activity compared to MTC cells (19), which may explain the increase in the number of MTLn3 cells collected into the needles containing matrigel compared to that for MTC cells.

Both EGF and TGF- α are growth factors found in mammary tissue. MTLn3 cells have around 50,000 EGF receptors/cell, while EGF receptors on the MTC cells are not detectable (8). By using EGF as the chemoattractant, we were able to selectively collect 15 times as many metastatic MTLn3 cells from MTLn3-derived metastatic primary tumors as MTC cells from MTC-derived non-metastatic tumors. Serum, which contains many growth factors with potential chemotactic activity, also stimulated the collection of tumor cells from MTLn3 tumors. Even though MTC cells show a motility response to serum, they were not collected with high efficiency into needles in response to serum indicating that additional factors besides motility are required for the large increase in the number of MTLn3 cells collected in response to serum.

Morphologically, MTC cells are elongated and polarized both *in vivo* and *in vitro* while the MTLn3 cells are generally unpolarized both in culture and in the primary tumor (10, 11). This difference is most dramatically illustrated by using intravital imaging techniques where GFP-expressing tumor cells are imaged directly in the primary tumor (8, 11). *In vivo*, MTLn3 cells are highly polarized around and oriented toward the blood vessels running through the primary tumor. MTC cells, on the other hand, are polarized throughout the tumor but the polarity is randomly oriented relative to vessels (11).

Characterization of the cells *in vitro* confirms the differences between the two cell-lines. In cultures that have not been stimulated with a chemoattractant, MTC cells locomote in a linear direction at approximately twice the velocity of MTLn3. MTLn3 cells, under these conditions are unpolarized and move in random directions or not at all (10). Upon stimulation with an EGF gradient, the MTLn3 cells become polarized and move linearly at approximately the same speed as the MTC cells, yet have the ability to reorient themselves to follow an EGF gradient with precision (9) a property not seen in MTC cells.

In vivo, in the primary tumor, both cell types move linearly at approximately the same speeds, but the MTLn3 cells tend to move only when they are polarized and in association with a vessel, while MTC cells can be seen moving throughout the tumor (8, 11). The ability of the MTLn3 cells to invade into a needle filled with matrigel in response to growth factors is fully consistent with the chemotactic motility exhibited by these cells *in vitro*, their polarity and locomotion toward vessels *in vivo*, and with the dramatically increased efficiency of intravasation measured as blood burden of tumor cells *in vivo* (11). This suggests that chemotaxis may be the key aspect of cell motility that contributes to invasion and intravasation. It also suggests that needles filled with growth factors and matrigel, when inserted into the primary tumor, can faithfully mimic the environment that supports invasion and intravasation *in vivo*, and that the same cell behaviors that contribute to chemotaxis *in vitro* also contribute to invasion *in vivo*.

An advantage of using the needle collection technique described here for the collection of cells for genomic/proteomic analysis is that the cell behavior can be characterized during the collection process. This can be done by varying the conditions

required for cell collection such as the extracellular matrix composition and/or cytokines used as chemoattractants, determining how these changes affect efficiency of cell collection, and then relating these observations to the gene expression and protein composition patterns subsequently obtained from array analysis of the collected cells. Furthermore, cells can also be characterized by intravital imaging during collection to directly visualize the cell-cell and cell-extracellular matrix interactions that contribute to the invasion of the needle under these different conditions. Finally, by comparing the gene expression patterns of cells collected by invasion into needles with that of cells obtained from the whole primary tumor, the blood and whole metastatic tumors, genes that contribute to the invasive process uniquely may be identified.

References

1. Fidler, I.J. (1999) Critical determinants of cancer metastasis: rationale for therapy. *Cancer Chemother Pharmacol*, 43 *Suppl*: S3-10.
2. Price, J.T., Bonovich, M.T., and Kohn, E.C. (1997) The biochemistry of cancer dissemination. *Crit Rev Biochem Mol Biol*, 32: 175-253.
3. Bonner, R.F., Emmert-Buck, M., Cole, K., Pohida, T., Chuaqui, R., Goldstein, S., and Liotta, L.A. (1997) Laser capture microdissection: molecular analysis of tissue. *Science* 278: 1481-1483.
4. Morris, V.L., Schmidt, E.E., MacDonald, I.C., Groom, A.C., and Chambers, A.F. (1997) Sequential steps in hematogenous metastasis of cancer cells studied by in vivo videomicroscopy. *Invasion Metastasis*, 17: 281-296.
5. Naumov, G.N., Wilson, S.M., MacDonald, I.C., Schmidt, E.E., Morris, V.L., Groom, A.C., Hoffman, R.M., and Chambers, A.F. (1999) Cellular expression of green fluorescent protein, coupled with high-resolution in vivo videomicroscopy, to monitor steps in tumor metastasis. *J Cell Sci*, 112: 1835-1842.
6. Stetler-Stevenson, W. G., Aznavoorian, S., and Liotta, L. A., (1993) Tumor cell interactions with the extracellular matrix during invasion and metastasis. *Annual Review of Cell Biology*, 9:541-574.
7. Kaufmann, A.M., Khazaie, K., Wiedemuth, M., Rohde-Schulz, B., Ullrich, A., Schirrmacher, V., and Lichtner, R.B. (1995) Expression of epidermal growth factor receptor correlates with metastatic potential of 13762NF rat mammary adenocarcinoma cells. *Int. J. Oncol.*, 4: 1149-1155.
8. Farina, K.L., Wyckoff, J., Rivera, J., Lee, H., Segall, J.E., Condeelis, J.S., and Jones, J.G. (1998) Cell motility of tumor cells visualized in living intact primary tumors using green fluorescent protein. *Canc.Res.*, 58: 2528-2532.
9. Bailly, M., Yan, L., Whitesides, G., Condeelis, J., and Segall, J. (1998): Regulation of Protrusion Shape and Adhesion to a Substratum During Chemotactic Responses of Mammalian Carcinoma Cells. *Exp. Cell Res.*; 241:285-299.
10. Shestakova, E., Wyckoff, J., Jones, J., Singer, R., and Condeelis, J. (1999) Correlation of β -Actin Messenger RNA Localization with Metastatic Potential in Rat Adenocarcinoma Cell Lines. *Cancer Res.*; 59: 1202-1205.

11. Wyckoff, J., Jones, J., Condeelis, J., and Segall, J. (2000) A Critical Step in Metastasis: *In vivo* Analysis of Intravasation at the Primary Tumor. *Cancer Res. Canc. Res.* (in press)
12. Segall, J.E., Tyrech, S., Boselli, L., Masseling, S., Helft, J., Chan, A., Jones, J., and Condeelis, J. (1996) EGF stimulates lamellipod extension in metastatic mammary adenocarcinoma cells by an actin-dependent mechanism. *Clin.Exp.Met.*, *14*: 61-72.
13. Glaves, D. (1986) Detection of circulating metastatic cells. *Prog Clin Biol Res*, *212*: 151-167.
14. Butler, T.P. and Gullino, P.M. (1975) Quantitation of cell shedding into efferent blood of mammary adenocarcinoma. *Cancer Res*, *35*: 512-516.
15. Liotta, L.A., Kleinerman, J., and Saidel, G.M. (1974) Quantitative relationships of intravascular tumor cells, tumor vessels, and pulmonary metastases following tumor implantation. *Cancer Res.*, *34*: 997-1004.
16. Welch, D.R., Neri, A., Nicolson, G.L. (1983) Comparison of 'spontaneous' and 'experimental' metastasis using rat 13762 mammary adenocarcinoma metastatic cell clones. *Inv. Met.* *3*: 65-80.
17. Yamamura, K., Kibbey, M.C., Jun, S.H., and Kleinman, H.K. (1993) Effect of matrigel and laminin peptide YIGSR on tumor growth and metastasis. *Semin. Cancer Biol.* *4*: 259-265.
18. Kibbey, M.C., Grant, D.S., and Klienmann, H.K. (1992) Role of the SIKVAV site of laminin in promotion of angiogenesis and tumor growth: an *in vivo* matrigel model. *J. Natl. Cancer Inst.* *84*: 1633-1638.
19. McGuire, P.G., and Seeds, M.W. (1989) The interaction of plasminogen activator with a reconstituted basement membrane matrix and extracellular macromolecules produced by cultured epithelial cells. *J. Cell. Biochem.* *40*: 215-227.
20. Nakajima, M., Welch, D.R., Belloni, P.N., and Nicolson, G.L. (1987) Degradation of basement membrane type IV collagen and lung subendothelial matrix by rat mammary adenocarcinoma cell clones of differing metastatic potentials. *Cancer Research* *47*: 4869-4876.

Figure Legends

Figure 1: Tumor cells are collected into matrigel-containing needles in response to EGF. Cells in culture were collected in needles containing matrigel and differing concentrations of EGF. The maximal number of cells was collected into the needle containing 25 nM EGF. Cell numbers were normalized to MTLn3 cells collected with Matrigel in buffer. The error bars shown are the SEM of 3 experiments.

Figure 2: Tumor cells chemotax toward needles containing EGF. Cells are seen orienting and moving towards a needle containing matrigel and 25 nM EGF. By 1.5 h after the needle was placed in the culture dish, cells 1 and 2 have already oriented themselves toward and have moved in the direction of the needle, while cell 3 has entered the field of view. By three hours, cells 1 and 2 have reached the matrigel edge. The edge of the matrigel (*) is delineated by the white line and shown in gray. Only motile cells within the field are numbered. The average velocity of the cells is $0.32 \pm 0.03 \mu\text{m}/\text{min}$.

Figure 3: Method for using needles for *in vivo* cell collection. Needles (125 μm I.D.) filled with matrigel and buffer, 25 nM EGF, or 10% FBS are shown placed in 25-gauge guide needles that are inserted into the primary tumor of an anesthetized rat.

Figure 4: Metastatic cells (MTLn3) are more efficient than non-metastatic cells (MTC) at entering matrigel filled needles in response to EGF *in vivo*. Cells were collected from metastatic (MTLn3) and non-metastatic (MTC) tumors using the *in vivo* experiment shown in Figure 3. Maximum response was for cells from the metastatic

MTLn3 tumors into EGF and serum containing needles. Cells were collected above background from metastatic tumors in response to matrigel in buffer but not agarose. All counts were normalized to MTC cells collected with matrigel in buffer. The error bars shown are the SEM of 4 experiments.

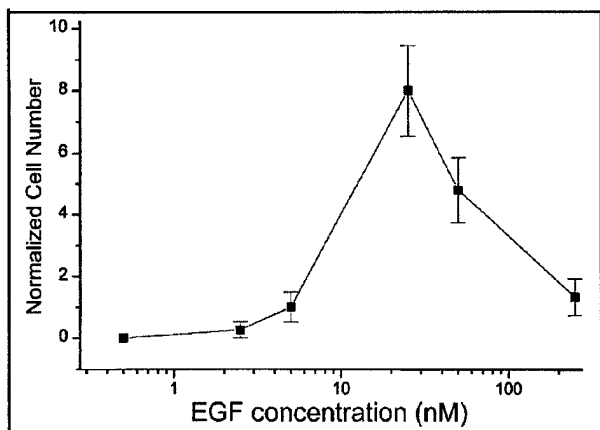


Figure 1

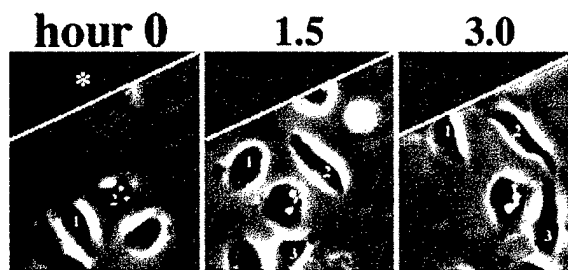


Figure 2

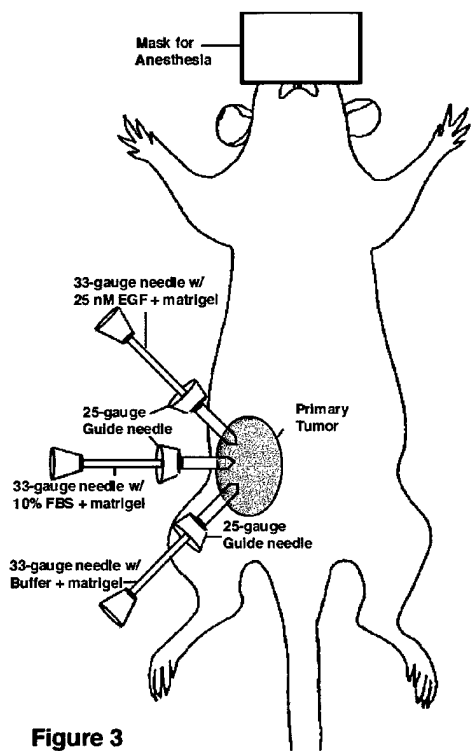


Figure 3

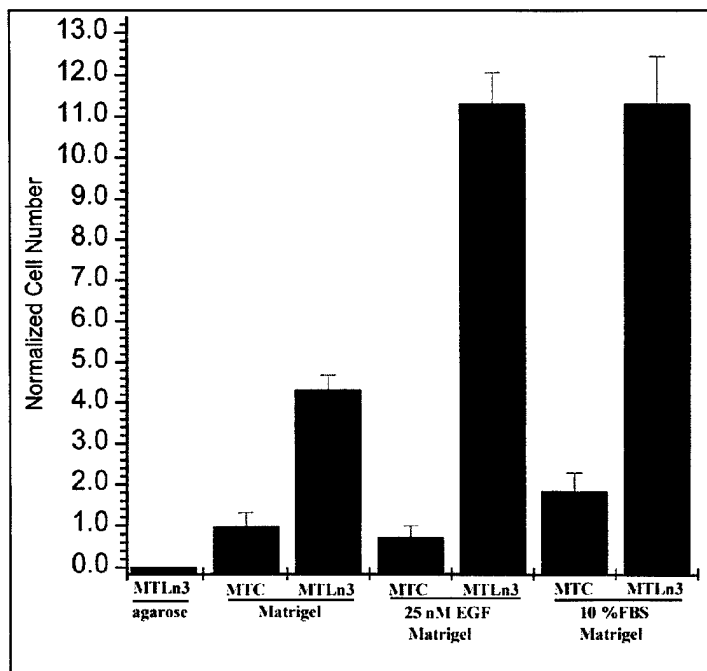


Figure 4

A Critical Step in Metastasis: *In Vivo* Analysis of Intravasation at the Primary Tumor¹

Jeffrey B. Wyckoff, Joan G. Jones, John S. Condeelis, and Jeffrey E. Segall²

Departments of Anatomy and Structural Biology [J. B. W., J. S. C., J. E. S.], Pathology [J. G. J.], and the Analytical Imaging Facility (J. S. C.), Albert Einstein College of Medicine, Bronx, New York 10461

ABSTRACT

Detailed evaluation of all steps in tumor cell metastasis is critical for evaluating the cell mechanisms controlling metastasis. Using green fluorescent protein transfectants of metastatic (MTLn3) and nonmetastatic (MTC) cell lines derived from the rat mammary adenocarcinoma 13762 NF, we have measured tumor cell density in the blood, individual tumor cells in the lungs, and lung metastases. Correlation of blood burden with lung metastases indicates that entry into the circulation is a critical step for metastasis. To examine cell behavior during intravasation, we have used green fluorescent protein technology to view these cells in time lapse images within a single optical section using a confocal microscope. *In vivo* imaging of the primary tumors of MTLn3 and MTC cells indicates that both metastatic and nonmetastatic cells are motile and show protrusive activity. However, metastatic cells show greater orientation toward blood vessels and larger numbers of host cells within the primary tumor, whereas nonmetastatic cells fragment when interacting with vessels. These results demonstrate that a major difference in intravasation between metastatic and nonmetastatic cells is detected in the primary tumor and illustrate the value of a direct visualization of cell properties *in vivo* for dissection of the metastatic process.

INTRODUCTION

Metastasis leads to poor prognosis in many cancer types. Metastasis of adenocarcinomas involves leaving the primary tumor either via lymphatics or blood vessels, transport to and arrest in a target organ, and growth of metastases in the target organ (1). Each of these steps is a multicomponent process, with potentially different tumor cell properties and molecules playing critical roles in different steps (2). As novel molecular methods are being developed to identify new genes and proteins that could contribute to specific steps, it is important to develop more detailed methods for the analysis of metastasis at the cellular level to accurately evaluate the roles of specific gene products in individual steps of metastasis. Similarly, as new therapies are developed, the effects of specific treatments on the individual steps in the metastatic cascade need to be evaluated.

The most common assays for metastatic ability *in vivo* have been end point assays. For example, *i.v.* injection of tumor cells (often termed "experimental metastasis"), followed by determination of the number of metastases in a target organ such as the lung, is a simple method for evaluation of arrest and growth of tumor cells in target organs (3). Detailed studies using this assay have demonstrated that extravasation *per se* tends not to be rate limiting, but that growth of metastases is inefficient (4, 5). However, this assay is limited by the introduction of a bolus (typically 100,000 cells) of *in vitro* cultivated

cells in a nonphysiological manner. A more physiological approach to analysis of tumor cell metastasis makes use of the injection of tumor cells into an appropriate (orthotopic) tissue, followed by growth of a primary tumor as the source of tumor cells for metastasis. Such "spontaneous metastasis" assays are more accurate models of human disease in that they rely on growth of a primary tumor, and the tumor cells themselves then must actively leave the primary tumor and enter the vasculature (6-8). Cell lines specifically selected for high metastatic ability through use of the experimental metastasis assay are not necessarily highly metastatic in the spontaneous metastasis assay (9). Thus, for a detailed comparison of all of the various steps of metastasis, an assay such as the spontaneous metastasis assay must be used.

However, analysis of metastasis using the spontaneous metastasis assay typically measures only the growth of the primary tumor and the number of metastases that form in a target organ. The relative efficiencies for various steps in this assay have never been directly determined. Such an analysis is crucial because of the heterogeneity of tumors and tumor cell lines. Human primary tumors show extensive variation in all properties, ranging from growth and morphology of primary tumors through tumor cell density in the blood and then formation and growth of metastases. Similarly, tumor cell lines show broad variation in formation of a primary tumor and metastatic ability. As specific cell lines are manipulated to express particular activated or inhibitory oncoproteins, the effects on metastatic abilities will need to be interpreted in terms of the particular steps in the metastatic cascade that are affected. Growth of the primary tumor is simple to quantify and has been an extremely useful assay for determining proteins that are important for tumor formation. However, entry of tumor cells into the circulation is the critical first step in the metastatic cascade, and although it has been assayed in various ways (10-12), it has not been observed directly.

Because for certain tumor types and conditions there are high levels of circulating tumor cells (13, 14), it has sometimes been assumed that entry into the circulation is not a critical step in tumor cell metastasis and that formation of metastases in target organs is rate limiting. Some studies using cell-based assays indicate that tumor cell burden in the blood can correlate with poor prognosis (15, 16). However, PCR or antibody-based assays for tumor cells in the blood may not show as strong a correlation (17-20). Animal studies using well-characterized cell lines and controlled conditions are needed to evaluate the role of intravasation.

In this study, we describe a straightforward procedure for comparing intravasation, extravasation, and growth in target organs during metastasis. For two mammary adenocarcinomas, the metastatic MTLn3 and poorly metastatic MTC cell lines, we use this procedure to demonstrate that intravasation is important. We then use *in vivo* time lapse confocal microscopy of MTLn3 and MTC primary tumors expressing GFP³ to compare the behavior of metastatic and nonmetastatic cells relative to blood vessels. We find that although both metastatic and nonmetastatic cells are motile in the primary tumor, metastatic cells are polarized toward blood vessels and nonmetastatic

Received 8/27/99; accepted 3/14/00.

The costs of publication of this article were defrayed in part by the payment of page charges. This article must therefore be hereby marked *advertisement* in accordance with 18 U.S.C. Section 1734 solely to indicate this fact.

¹ Supported by grants from the Department of Defense Army Breast Cancer Program [DAMD17-94-J-4314 (to J. E. S.) and DAMD17-96-1-6129 (to J. S. C.)] and a New York State Department of Health Empire Award (J. S. C.). J. E. S. is supported by an Established Scientist Award from the New York City affiliate of the American Heart Association.

² To whom requests for reprints should be addressed, at Department of Anatomy and Structural Biology, Albert Einstein College of Medicine, 1300 Morris Park Avenue, Bronx, NY 10461. Phone: (718) 430-4237; Fax: (718) 430-8996; E-mail: segall@accom.yu.edu.

³ The abbreviations used are: GFP, green fluorescent protein; EGF, epidermal growth factor.

cells tend to fragment during intravasation. These results provide new insights into the differences between metastatic and nonmetastatic cells and have implications for the types of assays that should be developed for prognosis.

MATERIALS AND METHODS

Cell Lines. MTLn3-GFP cells were used as described before (21). MTC-GFP cells were created using retroviral transfection of parental MTC cells with a GFP expression construct. The GFP sequence was excised from pEGFPN1 (Clontech) using NsiI and EcoRI and subcloned into the BamHI/EcoRI site of pLXSN. This construct was then transfected into Phoenix cells [supplied by Vaughn Latham and Rob Singer (AECOM, Bronx, NY)] using standard methods (22, 23) and allowed to grow overnight. The supernatant was collected, spun at 1000 rpm for 5 min, and 1 ml was overlaid on a confluent plate of MTC cells. Positive clones were selected by neomycin selection and GFP fluorescence. Stable cells were cultured the same as parental cells, as described previously (24). Cell growth rate and morphology of transfected cells was determined to be the same as parental cells, and fluorescence was shown to remain constant for 30 passages (data not shown). Extensive histopathology studies for the MTLn3-GFP cells (21) and the MTC-GFP cells were done to confirm that their metastatic potentials were similar to the parental cell lines.

Blood Burden, Single Cells in the Lung, and Metastases. Tumor cell blood burden was determined by placing a rat with a 6-week-old tumor under isoflurane anesthesia and removing 4 ml of blood from the right atrium via heart puncture. The blood was then spun at 5000 rpm for 5 min, and the serum layer and buffy coat region were plated into α -MEM growth medium. The following day, plates were rinsed twice with Dulbecco's PBS (Life Technologies, Inc.) to remove RBCs, and regular growth medium was added. After 6 days, all clones in the dish were counted. To test cell viability in the collection process, blood was drawn as above from noninjected rats. Cultured MTLn3-GFP and MTC-GFP cells were removed from growth dishes using trypsin/EDTA. Ten, 100, and 1000 tumor cells were added to 1 ml of blood and 1 ml of medium, respectively. The mixtures were then centrifuged, plated, and counted as described above for blood samples derived from rats bearing tumors. There was approximately 50% recovery of tumor cells from mixtures with blood as compared with mixtures with growth medium for both cell lines.

For visualization of single cells near the surface of the lungs, the lungs were removed after blood removal and euthanization of the rat. The lungs were then placed in matTek dishes (MatTek Corporation, Ashland, MA) with 1 ml of L15 medium (Life Technologies, Inc.) to keep them moist. Ten fields from each side of both major lobes were then visualized using a $\times 60$ objective on a Nikon inverted microscope. All whole single cells visible in these fields were counted. Tumor cells were shown to be countable by confirming their GFP fluorescence in the fluorescein channel and lack of fluorescence in the rhodamine channel of the Bio-Rad MRC-600 confocal microscope. A field is the 1.1-mm diameter visible area through the microscope oculars.

For measurement of metastases, excised lungs were placed in 3.7% formaldehyde, mounted in paraffin, sectioned, and stained with H&E. Slices were viewed using a $\times 20$ objective, and all visible metastases in a section containing more than five cells were counted.

Imaging of Living Tumors and Their Vasculature. Tumor imaging was performed as described previously (21). Briefly, 1×10^6 cells were injected under the second nipple anterior from the tail of a Fischer 344 rat and allowed to grow for 2.5 weeks. After 2.5 weeks, the rat was placed under isoflurane anesthesia and the tumor was exposed using a simple skin flap surgery, with as little disruption of the surrounding vasculature as possible. The animal was then placed onto a Bio-Rad MRC-600 confocal microscope, using a $\times 20$ objective and imaged in time lapse, with a single image being taken every minute. On average, about three different fields of each tumor were imaged for 20–30 min each.

For visualizing vasculature, 200 μ l of rhodamine-dextran (2 M dalton; Sigma Chemical Co.) at 20 mg/ml in Dulbecco's PBS was injected into the tail vein of the rat after anesthesia, but before surgery. The vasculature in the tumor was then visualized using the rhodamine channel of the Bio-Rad confocal.

Quantification of Images. Time lapse movies were reconstructed using NIH Image. Movies then were viewed and evaluated for the following criteria: (a) cell extension and retraction; (b) cell locomotion (21); (c) cell orientation

to the vasculature; and (d) host cell locomotion. Fields are defined as the visible area for each optical condition and are 2.4×10^5 square microns, unless indicated otherwise. For statistical purposes, an experiment is defined as a single tumor, and data are reported as the percentage of time lapse sequences for which a recorded event happens during an experiment. The velocity of cell locomotion was determined by the distance the cell moved between image frames.

Percent orientation in Table 2 was determined as the percentage of blood vessels in an imaging field with four or more directly adjacent cells polarized toward the vessel. Percent orientation was corrected for randomly polarized fields of cells by subtracting from the above value the percentage of blood vessels with both adjacent and nonadjacent cells polarized toward the vessel.

RESULTS

Entry into the Bloodstream Is an Important Step in Metastasis.

To provide a quantitative comparison between blood burden and lung metastasis during spontaneous metastasis, we made use of mammary adenocarcinoma cells stably expressing GFP. The metastatic MTLn3 and nonmetastatic MTC cell lines are both derived from the Fisher rat 13762 NF mammary adenocarcinoma (25). They were transfected with GFP expression vectors and the neomycin resistance selection marker, as described by Farina *et al.* (21) and in "Materials and Methods." The cells are uniformly fluorescent, and expression of GFP does not alter their metastatic properties (see Ref. 21 and below).

Cells were injected into the mammary fat pads of Fisher 344 rats and allowed to grow for 6 weeks. To determine blood burden before filtration by any capillary bed, but with minimal perturbation of the primary tumor, the rats were anesthetized, and 4 ml of blood was withdrawn from the right atrium of the heart. The cells in the serum and buffy coat were plated in growth medium and allowed to grow for 1 week. Tumor cell colonies were identified by cell morphology and GFP fluorescence. The blood of rats carrying MTLn3 primary tumors formed about 23 colonies/4 ml of blood, which was significantly more than the blood burden of <1 colony/4 ml for rats carrying MTC primary tumors ($P < 0.002$; Table 1, column 2). Control experiments using defined numbers of cells mixed with blood showed a 50% plating efficiency for both cell lines. Thus, there was a significantly larger number of viable tumor cells present in the blood of rats carrying MTLn3 tumors compared with the blood of rats carrying MTC tumors. This difference was not due to larger MTLn3 tumors (Table 1, column 1). MTC tumors tended to be larger than MTLn3 tumors.

GFP fluorescence was used to identify single cells present in the lungs of the same rats used to measure blood burden. After removal of the blood, the animals were euthanized and the lungs were dissected. The lungs were viewed using a confocal microscope, and the number of fluorescent cells present in 40 high power fields was determined for each animal. Only cells showing fluorescence in the GFP channel with no fluorescence in the rhodamine channel were counted. Rats carrying MTLn3 tumors had significantly more tumor cells present in the lungs than rats carrying MTC tumors ($P < 0.003$; Table 1, column 3). In addition, for rats carrying MTLn3 tumors, comparing blood burden and fluorescent cells in the lungs in each

Table 1 *In vivo* tumor cell distributions

For MTLn3, 15 rats received injections and for MTC, 8 rats received injections. Tumor cell distributions were measured, means and SEs of the mean were calculated, and statistical significance was evaluated using the nonparametric Wilcoxon test.

	Tumor size (cm ³)	Cells in blood (per 4 ml)	Cells in lungs (per 40 HPF)	Lung mets (per section)
MTLn3	31.0 \pm 5.5	22.8 \pm 13.6	35.7 \pm 10.1	17.9 \pm 13.6
MTC	44.5 \pm 9.9	0.25 \pm 0.16	0.75 \pm 0.75	0
<i>P</i>	<0.4	<0.002	<0.003	<0.003

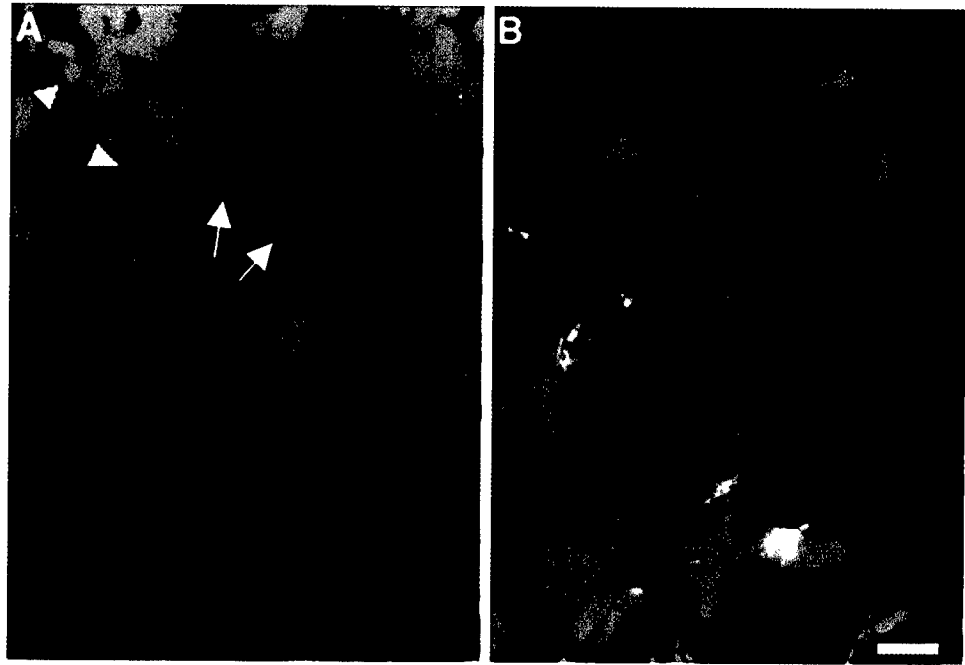


Fig. 1. MTLn3-GFP cells orient toward blood vessels, whereas MTC-GFP cells do not. Orientation of MTLn3-GFP cells (A) and MTC-GFP cells (B) to blood vessels in the primary tumor. A, MTLn3-GFP cells (green) near the vessel (red) are seen to orient themselves toward the vessel in an elongated fashion (arrows) as opposed to those away from the vessel (arrowheads). B, MTC-GFP cells (green) randomly associate with the vessel (red), and remain elongated away from the vessel. Bar, 25 μ m.

animal there was a significant correlation (correlation coefficient, 0.86; $P < 0.0004$). However, there were no correlations with the size of the primary tumor (correlation coefficient, 0.23–0.5; $P > 0.05$).

To evaluate metastases in the lungs of animals, sections of lungs were stained with H&E and evaluated for metastases. Rats carrying MTLn3 tumors had significantly more metastases than rats carrying MTC tumors ($P < 0.003$; Table 1, column 4). In addition, for rats carrying MTLn3 tumors there was a significant correlation between blood burden and metastases (correlation coefficient, 0.96; $P < 0.0001$).

In summary, from this analysis there was a clear correlation between tumor cell density in the blood and either numbers of single tumor cells in the lungs or metastases. This correlation was present both when comparing metastatic and nonmetastatic cell lines (MTLn3 and MTC) and when comparing MTLn3 tumors on the level of individual animals. To our knowledge, this is the first time that such a comparison has been performed on a single animal basis. The presence of a correlation between blood burden and both single cells, as well as metastases in the lungs, indicates that entry into the blood is important for metastasis of cells derived from the 13762 NF mammary adenocarcinoma. These data suggest that a more detailed analysis of cell behavior in the primary tumor is important for determining the properties that enable MTLn3 cells to gain access to the circulation. To perform such studies, we made use of the GFP expression of these cell lines to perform intravital imaging of the primary tumors.

Intravital Imaging of MTLn3 and MTC Primary Tumors

Metastatic Cells Are Oriented toward Blood Vessels. As reported previously (26), MTLn3-GFP cells form loose clusters of rounded, nonpolarized cells in the primary tumor, whereas MTC-GFP cells are elongated and polarized in tight sheets. This was confirmed by both histopathology sections and intravital imaging. However, around blood vessels, MTLn3-GFP cells were elongated and polarized toward blood vessels. In Fig. 1A, MTLn3-GFP cells (green) are elongated and polarized (arrows) toward the vessel (red), whereas cells away from the vessel are rounded (arrowheads). Fig. 1B shows MTC-GFP cells (green) that are elongated throughout the field of

view, with cell elongation occurring independent of the vessel positions. Overall, for MTLn3 tumors, 57 \pm 6% of all vessels had polarized cells near them, compared with 24 \pm 4% for vessels in MTC-GFP tumors (Table 2, column 1). This suggests that there is a vessel-mediated effect on MTLn3 cells that results in orientation toward the vessels.

The differences in cell locomotion (translocation) and protrusiveness between metastatic and nonmetastatic cells are much smaller in the primary tumor. During a time lapse sequence, cells within the primary tumor can be detected extending and retracting processes, as well as translocating. Both protrusiveness and translocation were reported previously for MTLn3-GFP cells in the primary tumor (21), and similar phenomena were observed in the MTC-GFP primary tumors. For the MTLn3-GFP tumors, cell protrusion and retraction occur in 62% of tumors compared with 47% for MTC tumors (Table 2, column 2). Fig. 2 shows the protrusive activity of an MTC-GFP tumor cell. The cell extends a small protrusion (Fig. 2B), which then enlarges (Fig. 2C). The movement of the leading edge of this cell was 3.8 μ m/min during maximum rate of extension, consistent with the average rate of movement seen for MTLn3 and MTC cells (see below). For MTLn3-GFP cells, the most obvious shape changes occur at the periphery of vessels where the cells are elongated, whereas for MTC cells protrusion and locomotion occur randomly relative to vessels.

Cell translocation occurs much less frequently in both tumor types. As opposed to protrusive activity, only a small fraction of the cells within a primary tumor translocate at a given time. MTLn3-GFP cell

Table 2. *In vivo* analysis of tumor cell behavior

The percentage of tumor time lapse sequences with cells showing the specified behavior is given, together with SE of the mean. Orientation was determined as the percentage of blood vessels in an imaging field with four or more adjacent cells polarized toward the vessel (see "Materials and Methods"). For MTLn3 tumors, a total of 122 fields from 45 tumors containing 163 vessels was analyzed. For MTC tumors, a total of 63 fields from 24 tumors with 97 vessels was analyzed.

	Orientation	Protrusion	Translocation	Fragmentation
MTLn3	57% \pm 6%	62% \pm 5%	17% \pm 4%	6% \pm 2%
MTC	24% \pm 4%	47% \pm 7%	10% \pm 4%	32% \pm 5%
<i>P</i>	<0.0001	<0.04	<0.07	<0.001

locomotion within the primary tumor, as reported previously and observed with more tumors here, is seen as a linear movement. The cell shown in Fig. 3 moves on a linear path at a speed of $3.6 \mu\text{m}/\text{min}$. This type of movement is seen in 17% of all MTLn3 tumors and 10% of MTC tumors (Table 2, column 3). The MTC-GFP cell shown in Fig. 4 moves at a rate of $3.6 \mu\text{m}/\text{min}$. The average velocities of movement of MTLn3 ($3.4 \mu\text{m}/\text{min}$, 12 cells) and MTC ($3.7 \mu\text{m}/\text{min}$, 7 cells) were similar.

Nonmetastatic Cells Demonstrate Extensive Fragmentation. MTC-GFP tumor cells show a significantly greater number of cell fragmentation events compared with MTLn3-GFP tumor cells. Fragments of cells are visualized breaking from cell protrusions and moving away at an accelerated rate of speed (Fig. 5). In Fig. 5, a fragment is seen attached to a cell extension (A), then breaks off and moves away from the cell (B and C). The initial rate of protrusion of the extension was $2.8 \mu\text{m}/\text{min}$, but the fragment speed of movement is $11\text{--}15 \mu\text{m}/\text{min}$. This was observed in 32% of MTC-GFP tumors

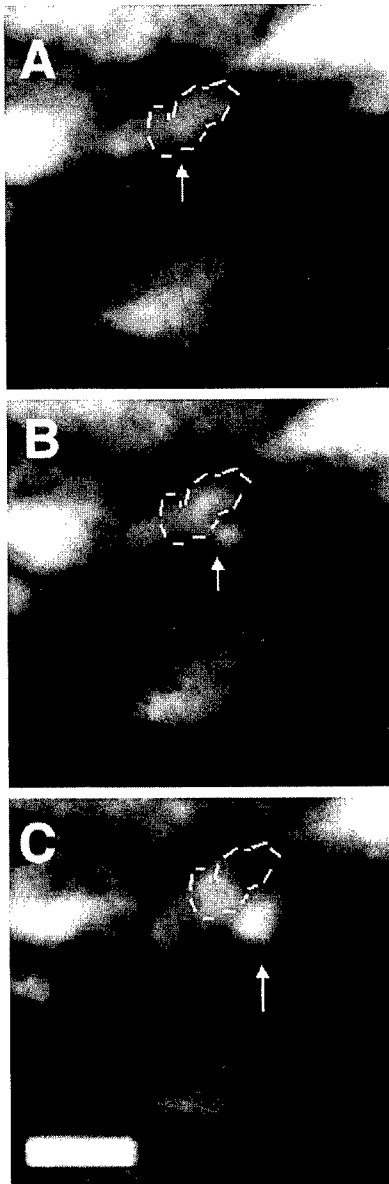


Fig. 2. MTC-GFP cells are able to move in a primary tumor by first sending out a thin leading edge protrusion through a small space. Protrusive movement of a whole MTC-GFP cell within the primary tumor viewed in a single optical section *in situ*. A, initial position of cell. B, initial extension of protrusion. C, further protrusion. The outline shows starting position. The images are 5 min apart. Bar, $25 \mu\text{m}$.



Fig. 3. MTLn3-GFP cells exhibit linear translocation *in situ*. Movement of a MTLn3-GFP cell in a single optical section of the primary tumor. The cell moved over a distance of $22 \mu\text{m}$. A, the cell seen in its starting position (outlined, with arrow). B, cell has moved to a new position 6 min later (arrow). Its starting position is outlined. The cell moved at an average velocity of $3.6 \mu\text{m}/\text{min}$. Bar, $25 \mu\text{m}$.

compared with 6% of MTLn3-GFP tumors (Table 2, column 4). In a number of cases, the fragmentation was seen to occur in blood vessels. The higher velocity of the fragment is consistent with passive flow in the blood because the velocity is too high for cell locomotion (maximum about $4 \mu\text{m}/\text{min}$) and close to the velocity of blood flow in small vessels.

More Motile Host Cells Are Visualized in Metastatic Tumors. During fluorescent imaging of GFP-tagged tumor cells, we have observed nonfluorescent cells moving against the fluorescent tumor cell background as they block and scatter fluorescence from the tumor cells (Fig. 6). It is likely that these are host immune system cells for the following reasons: (a) the cells are not fluorescent; (b) the cells are smaller than the tumor cells; and (c) the speed of movement is relatively high (on the order of $10 \mu\text{m}/\text{min}$). Although host cells were observed at similar frequencies in MTLn3 and MTC tumors (28% and 23%, respectively; Table 3, column 1), there was a significant difference in the number of host cells observed. For MTLn3-GFP tumors, there was an average of 11 host cells observed per field, compared with 2 host cells/field for MTC-GFP tumors (Table 3, column 2). The increased numbers of host cells may aid in either polarizing the tumor cells toward blood vessels or in generating pores through which tumor cells can intravasate.

Movies of the data from which the figures were derived are available.⁴

DISCUSSION

We present here the combination of two novel analyses of tumor cell metastasis: (a) a steady-state analysis of tumor cell distributions in individual animals; and (b) *in vivo* imaging of cell behavior in primary tumors. The steady-state analysis of tumor cell distributions indicates that entry into the vasculature is an important step that contributes to differences in metastasis between MTLn3- and MTC-

⁴ <http://www.aecom.yu.edu/asb/segall/segall.htm>.

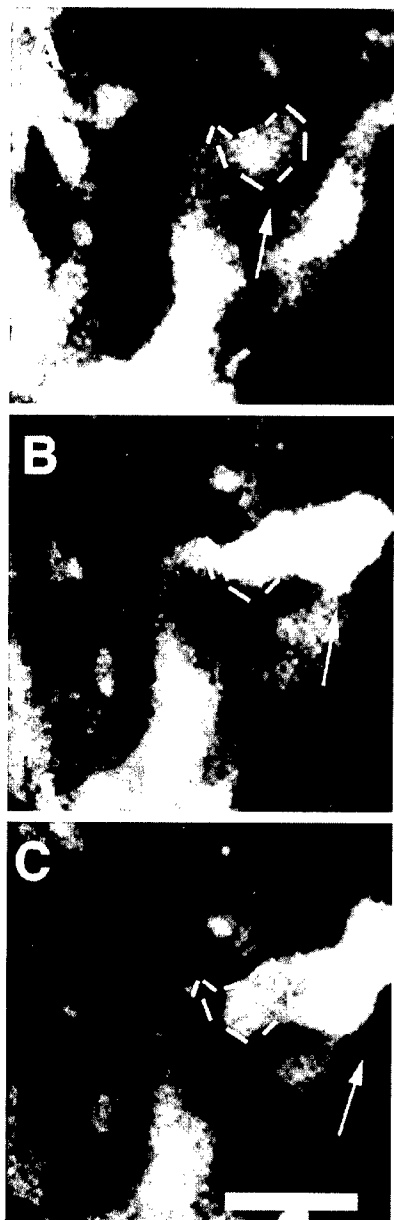


Fig. 4. MTC-GFP cells exhibit linear translocation *in situ*. Movement of a MTC-GFP cell in a single optical section of the primary tumor. A, cell is shown outlined in its starting position (arrow). B and C, images showing a progressively linear movement (arrows). The outline shows the original position. The cell moved at an average speed of 3.6 $\mu\text{m}/\text{min}$. The images are 4 min apart. Bar, 25 μm .

derived tumors. To define the mechanisms behind this difference, we used confocal microscopy of GFP-transfected cells in anesthetized animals. MTLn3 tumor cells were more highly oriented around blood vessels compared with MTC tumor cells. Protrusive activity and random cell movement were similar. However, MTC tumor cells were much more likely to form fragments. In addition, more host cells were detected in MTLn3 tumors compared with MTC tumors.

Steady-State Analysis of Metastasis. We have used a steady-state analysis of tumor cell distributions in individual animals to develop a general method for comparing intravasation with growth in the lungs during metastasis. We have found that although the primary tumor sizes formed are similar, rats carrying the more metastatic MTLn3 tumors have about 90 times more cells in the blood than rats carrying MTC tumors. Although previous studies had demonstrated that MTC cells injected *i.v.* form few metastases in the lungs (27), this is the first

demonstration that MTC cells are also unable to effectively enter the circulation.

There are two limitations in our estimate of tumor cell density in the blood. First, because we are using colony counts, each clump of tumor cells would be counted as a single colony-forming unit, or cell (10, 12, 14). Second, the cells must be able to grow *in vitro*. Given that these tumor cell lines grow well *in vitro* before injection into the animal to form a tumor, the latter limitation is not significant. Reconstruction experiments *in vitro* indicate that exposure to blood *per se* produces a roughly 50% reduction in plating efficiency for both cell lines. Thus, our estimate of tumor cell density in the blood may be an underestimate of the true number.

To determine whether metastasis of the MTLn3 cells could be dependent on intravasation as well, we compared the tumor cell density in the blood with single cells and metastases in the lungs for each rat carrying MTLn3 tumors. We found a significant correlation between blood density and single cells or metastases in the lungs. This result suggests that entry into or survival in the vasculature is an inefficient step for MTLn3 cells as well as for MTC cells. In addition, for animals carrying MTLn3 tumors, the number of lung metastases is

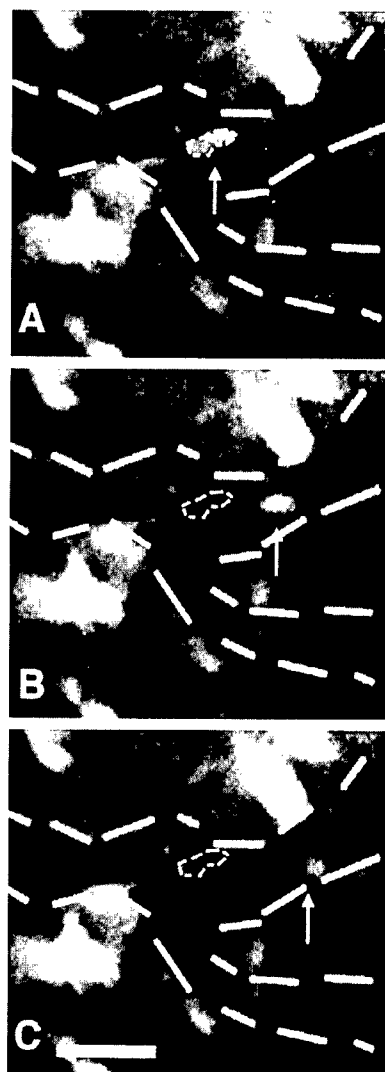


Fig. 5. The protrusions of MTC-GFP cells *in situ* are seen to break off from the cell body and move away rapidly. A, cell protrusion before being broken off (arrow). B and C, fragment broken off from the protrusion (arrows). The outline shows starting position. Speed of fragment after breaking away from protrusion suggests movement into vascular flow (large hash marks delineate vessel). The initial speed of protrusion is 2.8 $\mu\text{m}/\text{min}$; after release it increases to 11–15 $\mu\text{m}/\text{min}$. The images are 1 min apart. Bar, 25 μm .

less than would be expected given the single cell density in the lungs. This indicates that growth of metastases in the lungs is also inefficient, as has been well recognized (28–32).

In Vivo Imaging of the Primary Tumor. Given the results above indicating that intravasation is an important difference between metastatic and nonmetastatic tumors, a more detailed analysis of the cell behavior in the primary tumor becomes important. A number of researchers have made use of GFP (5, 21, 33–35) or lacZ (36–40) expression to increase the sensitivity of observations of disseminated tumor cells in target organs. We made use of techniques developed to follow individual tumor cells in primary tumors with an intact blood supply. By using a confocal scanning microscope to image cells that stably express green fluorescent protein, we are able to follow cell movements over 30 min. These studies provide the first comparison of *in vivo* cell behavior at the primary tumor with metastatic ability.



Fig. 6. Host cells can be visualized as shadows on top of white fluorescent cells in the primary tumor. Host cell movement over MTLn3-GFP cells in a single optical section of the primary tumor viewed *in situ*. A–C, host cells are seen as black shapes (arrows) moving over fluorescent tumor cells (MTLn3-GFP). The outline shows the starting position. Host cells move at 7.7 $\mu\text{m}/\text{min}$, and the images are 7 min apart. Bar, 25 μm .

Table 3 Host cells in tumor

The percentage of tumor time lapse sequences with cells showing the specified behavior is given, together with SE of the mean. For MTLn3 tumors, a total of 122 fields from 45 tumors was analyzed. For MTC tumors, a total of 63 fields from 24 tumors was analyzed.

	Tumors with host cells visualized	Number of host cells per field
MTLn3	28% \pm 5%	11.18 \pm 1.33
MTC	23% \pm 6%	1.8 \pm 0.19
P	<0.45	<1 \times 10 ⁻⁸

There are three major differences between the MTLn3 and MTC primary tumors: increased cell orientation toward blood vessels in MTLn3 tumors, increased fragmentation of cells in MTC tumors, and increased numbers of putative host cells in MTLn3 tumors. There are not as dramatic differences in protrusive activity and random cell translocation between these tumors.

Increased cell orientation of MTLn3 cells toward blood vessels could increase the efficiency with which they can then intravasate. The increased orientation could result in directed movement into the blood vessel and more cells moving into the blood. The orientation could be induced by chemoattractant diffusing from the blood vessel. Growth factors, including EGF or platelet-derived growth factor, are present in platelets and smooth muscle cells (*e.g.*, see Refs. 41–44). Release of growth factors from these cells or endothelial cells could provide a gradient that would produce a chemotactic response. MTLn3 cells are chemotactic toward EGF *in vitro*, whereas MTC cells are not (45). MTLn3 cells express more EGF receptors than MTC cells (46), and expression of the EGF receptor in MTC cells increases chemotactic responses to EGF and metastatic ability (47, 48). Expression of the EGF receptor and other EGF receptor homologues, such as ErbB2, have been correlated with poor prognosis. It is possible that chemotactic signaling mediated by the EGF receptor is important in enhancing metastatic capability in addition to the well characterized effects of EGF receptor signaling on mitogenesis.

The increased fragmentation of MTC cells compared with MTLn3 cells provides an additional mechanism by which viable cell number in the blood might be low for MTC cells. In some cases, we have identified fragmentation occurring during intravasation. If the shear forces in the blood vessels are causing MTC cells to fragment as they enter the blood vessel, that event will eliminate the possibility of metastasis. The increased susceptibility to fragmentation of MTC cells could reflect a lack of orientation toward the blood vessel and slow traversal of the endothelium due to a reduced chemotactic response, as suggested above. Morris *et al.* (49) have reported fragmentation of tumor cells injected *i.v.* and then viewed during extravasation into microvascular beds. At the extravasation stage of metastasis, fragmentation of both metastatic and nonmetastatic cells may occur if cells do not rapidly polarize and exit the blood vessel.

The observation of fragmentation of poorly metastatic cells has important implications for biochemical or molecular-based assays of blood. Given that cell fragments would contain tumor protein and DNA, immunological assays for tumor proteins or PCR-based assays for tumor DNA would be positive, although the fragments would be unable to metastasize. In that event, PCR- or protein-based assays of blood samples might not be useful for predicting metastases. A cell-based assay that evaluates the size of cells may be a more powerful predictor of poor prognosis.

An unexpected dividend of the GFP-based imaging was the ability to image motile nonfluorescent cells against the background of fluorescent cells. We have observed small, rapidly moving cells that are likely to be host immune cells. H&E sections of the primary tumor confirm that host immune cells are present in the primary tumor (data

not shown), supporting this interpretation. Increased numbers of immune system cells could contribute to increased metastasis by production of chemotactic factors or degradation of extracellular matrix barriers (e.g., see Refs. 50–54).

Breast cancer both in humans and in animal models including the MTLn3 cells (21, 55) spreads to lymph nodes, indicating that the lymphatic circulation can also be important for tumor cell metastasis. In our *in vivo* studies, in cases in which tumor cells are oriented or exiting the tumor in the absence of a labeled blood vessel, it is possible that the cells are interacting with lymphatics. Comparing the *in vivo* behavior of tumor cells around lymphatics with their behavior around blood vessels awaits development of an appropriate *in vivo* marker for lymphatics.

In summary, we have demonstrated a method for providing a more detailed analysis of metastatic ability of tumor cells. The method is straightforward and should be valuable in determining the contributions to metastasis of specific proteins expressed in tumor cells. In addition, our *in vivo* analysis of tumor cell behavior has indicated that cell orientation toward blood vessels may be a characteristic of metastatic cells and that poorly metastatic cells can fragment during intravasation. These distinctions may prove important in choosing appropriate assays for predicting disease progression.

ACKNOWLEDGMENTS

We gratefully acknowledge the staff of the Analytical Imaging Facility at Albert Einstein College of Medicine for assistance in intravital imaging and image analysis, Dr. Maryse Bailly for aid in the generation of rat tumors, and the laboratories of Drs. John S. Condeelis and Jeffrey E. Segall for scientific and critical input.

REFERENCES

- Fidler, I. J. Critical determinants of cancer metastasis: rationale for therapy. *Cancer Chemother. Pharmacol.*, **43** (Suppl.): S3–S10, 1999.
- Price, J. T., Bonovich, M. T., and Kohn, E. C. The biochemistry of cancer dissemination. *Crit. Rev. Biochem. Mol. Biol.*, **32**: 175–253, 1997.
- Price, J. E. The biology of cancer metastasis. *Prog. Clin. Biol. Res.*, **354A**: 237–255, 1990.
- Morris, V. L., Schmidt, E. E., MacDonald, I. C., Groom, A. C., and Chambers, A. F. Sequential steps in hematogenous metastasis of cancer cells studied by *in vivo* videomicroscopy. *Invasion Metastasis*, **17**: 281–296, 1997.
- Naumov, G. N., Wilson, S. M., MacDonald, I. C., Schmidt, E. E., Morris, V. L., Groom, A. C., Hoffman, R. M., and Chambers, A. F. Cellular expression of green fluorescent protein, coupled with high-resolution *in vivo* videomicroscopy, to monitor steps in tumor metastasis. *J. Cell Sci.*, **112**: 1835–1842, 1999.
- Kerbel, R. S. What is the optimal rodent model for anti-tumor drug testing? *Cancer Metastasis Rev.*, **17**: 301–304, 1998.
- Killian, J. J., Radinsky, R., and Fidler, I. J. Orthotopic models are necessary to predict therapy of transplantable tumors in mice. *Cancer Metastasis Rev.*, **17**: 279–284, 1998.
- Price, J. E. Analyzing the metastatic phenotype. *J. Cell. Biochem.*, **56**: 16–22, 1994.
- Weiss, L., Mayhew, E., Rapp, D. G., and Holmes, J. C. Metastatic inefficiency in mice bearing B16 melanomas. *Br. J. Cancer*, **45**: 44–53, 1982.
- Glaves, D. Detection of circulating metastatic cells. *Prog. Clin. Biol. Res.*, **212**: 151–167, 1986.
- Butler, T. P., and Gullino, P. M. Quantitation of cell shedding into efferent blood of mammary adenocarcinoma. *Cancer Res.*, **35**: 512–516, 1975.
- Liotta, L. A., Kleinerman, J., and Saitel, G. M. Quantitative relationships of intravascular tumor cells, tumor vessels, and pulmonary metastases following tumor implantation. *Cancer Res.*, **34**: 997–1004, 1974.
- Tarin, D., Price, J. E., Kettlewell, M. G., Souter, R. G., Vass, A. C., and Crossley, B. Mechanisms of human tumor metastasis studied in patients with peritoneovenous shunts. *Cancer Res.*, **44**: 3584–3592, 1984.
- Glaves, D., Huben, R. P., and Weiss, L. Haematogenous dissemination of cells from human renal adenocarcinomas. *Br. J. Cancer*, **57**: 32–35, 1988.
- Racila, E., Euhus, D., Weiss, A. J., Rao, C., McConnell, J., Terstappen, L. W. M. M., and Uhr, J. W. Detection and characterization of carcinoma cells in the blood. *Proc. Natl. Acad. Sci. USA*, **95**: 4589–4594, 1998.
- Denis, M. G., Lipart, C., Leborgne, J., LeHur, P. A., Galmiche, J. P., Denis, M., Ruud, E., Truchaud, A., and Lustenberger, P. Detection of disseminated tumor cells in peripheral blood of colorectal cancer patients. *Int. J. Cancer*, **74**: 540–544, 1997.
- Kawamata, H., Uchida, D., Nakashiro, K., Hino, S., Omotahara, F., Yoshida, H., and Sato, M. Haematogenous cytokeratin 20 mRNA as a predictive marker for recurrence in oral cancer patients. *Br. J. Cancer*, **80**: 448–452, 1999.
- Gao, C. L., Maheshwari, S., Dean, R. C., Tatum, L., Mooneyhan, R., Connelly, R. R., McLeod, D. G., Srivastava, S., and Moul, J. W. Blinded evaluation of reverse transcriptase-polymerase chain reaction prostate-specific antigen peripheral blood assay for molecular staging of prostate cancer. *Urology*, **53**: 714–721, 1999.
- de la Taille, A., Olsson, C. A., and Katz, A. E. Molecular staging of prostate cancer: dream or reality? *Oncology (Basel)*, **13**: 187–194, 1999.
- Peck, K., Sher, Y. P., Shih, J. Y., Roffler, S. R., Wu, C. W., and Yang, P. C. Detection and quantitation of circulating cancer cells in the peripheral blood of lung cancer patients. *Cancer Res.*, **58**: 2761–2765, 1998.
- Farina, K. L., Wyckoff, J., Rivera, J., Lee, H., Segall, J. E., Condeelis, J. S., and Jones, J. G. Cell motility of tumor cells visualized in living intact primary tumors using green fluorescent protein. *Cancer Res.*, **58**: 2528–2532, 1998.
- Miller, A. D., and Rosman, G. J. Improved retroviral vectors for gene transfer and expression. *Biotechniques*, **7**: 980–982, 1989.
- Kinsella, T. M., and Nolan, G. P. Episomal vectors rapidly and stably produce high-titer recombinant retrovirus. *Hum. Gene Ther.*, **7**: 1405–1413, 1996.
- Segall, J. E., Tyerech, S., Boselli, L., Masseling, S., Helft, J., Chan, A., Jones, J., and Condeelis, J. EGF stimulates lamellipod extension in metastatic mammary adenocarcinoma cells by an actin-dependent mechanism. *Clin. Exp. Metastasis*, **14**: 61–72, 1996.
- Neri, A., Welch, D., Kawaguchi, T., and Nicolson, G. L. Development and biologic properties of malignant cell sublines and clones of a spontaneously metastasizing rat mammary adenocarcinoma. *J. Natl. Cancer Inst.*, **68**: 507–517, 1982.
- Shestakova, E. A., Wyckoff, J., Jones, J., Singer, R. H., and Condeelis, J. Correlation of β -actin messenger RNA localization with metastatic potential in rat adenocarcinoma cell lines. *Cancer Res.*, **59**: 1202–1205, 1999.
- Welch, D. R., Neri, A., and Nicolson, G. L. Comparison of “spontaneous” and “experimental” metastasis using rat 13762 mammary adenocarcinoma metastatic cell clones. *Invasion Metastasis*, **3**: 65–80, 1983.
- Glaves, D. Correlation between circulating cancer cells and incidence of metastases. *Br. J. Cancer*, **48**: 665–673, 1983.
- Weiss, L., and Ward, P. M. Lymphogenous and hematogenous metastasis of Lewis lung carcinoma in the mouse. *Int. J. Cancer*, **40**: 570–574, 1987.
- Liotta, L. A., and DeLisi, C. Method for quantitating tumor cell removal and tumor cell-invasive capacity in experimental metastases. *Cancer Res.*, **37**: 4003–4008, 1977.
- Koop, S., Schmidt, E. E., MacDonald, I. C., Morris, V. L., Khokha, R., Grattan, M., Leone, J., Chambers, A. F., and Groom, A. C. Independence of metastatic ability and extravasation: metastatic ras-transformed and control fibroblasts extravasate equally well. *Proc. Natl. Acad. Sci. USA*, **93**: 11080–11084, 1996.
- Lin, W. C., Pretlow, T. P., Pretlow, T. G., and Culp, L. A. Development of micrometastases: earliest events detected with bacterial lacZ gene-tagged tumor cells. *J. Natl. Cancer Inst.*, **19**: 82: 1497–1503, 1990.
- Chishima, T., Miyagi, Y., Wang, X., Baranov, E., Tan, Y., Shimada, H., Moossa, A. R., and Hoffman, R. M. Metastatic patterns of lung cancer visualized live and in process by green fluorescence protein expression. *Clin. Exp. Metastasis*, **15**: 547–552, 1997.
- Kan, Z., and Liu, T. J. Video microscopy of tumor metastasis: using the green fluorescent protein (GFP) gene as a cancer-cell-labeling system. *Clin. Exp. Metastasis*, **17**: 49–55, 1999.
- Hoffman, R. M. Orthotopic transplant mouse models with green fluorescent protein-expressing cancer cells to visualize metastasis and angiogenesis. *Cancer Metastasis Rev.*, **17**: 271–277, 1998.
- Kobayashi, K., Nakanishi, H., Inada, K., Fujimitsu, Y., Yamachika, T., Shirai, T., and Tatematsu, M. Growth characteristics in the initial stage of micrometastasis formation by bacterial LacZ gene-tagged rat prostatic adenocarcinoma cells. *Jpn. J. Cancer Res.*, **87**: 1227–1234, 1996.
- McLeskey, S. W., Zhang, L., Kharbanda, S., Kurebayashi, J., Lippman, M. E., Dickson, R. B., and Kern, F. G. Fibroblast growth factor overexpressing breast carcinoma cells as models of angiogenesis and metastasis. *Breast Cancer Res. Treat.*, **39**: 103–117, 1996.
- Kruger, A., Schirmacher, V., and Khokha, R. The bacterial lacZ gene: an important tool for metastasis research and evaluation of new cancer therapies. *Cancer Metastasis Rev.*, **17**: 285–294, 1998.
- Culp, L. A., Lin, W. C., Kleinman, N. R., Campero, N. M., Miller, C. J., and Holleran, J. L. Tumor progression, micrometastasis, and genetic instability tracked with histochemical marker genes. *Prog. Histochem. Cytochem.*, **33**: 11–15, 1998.
- Kobayashi, K., Nakanishi, H., Masuda, A., Tezuka, N., Mutai, M., and Tatematsu, M. Sequential observation of micrometastasis formation by bacterial lacZ gene-tagged Lewis lung carcinoma cells. *Cancer Lett.*, **112**: 191–198, 1997.
- Calabro, A., Orsini, B., Renzi, D., Papi, L., Surrenti, E., Amorosi, A., Herbst, H., Milani, S., and Surrenti, C. Expression of epidermal growth factor, transforming growth factor- α and their receptor in the human oesophagus. *Histochem. J.*, **29**: 745–758, 1997.
- Peoples, G. E., Blotnick, S., Takahashi, K., Freeman, M. R., Klagsbrun, M., and Eberlein, T. J. T lymphocytes that infiltrate tumors and atherosclerotic plaques produce heparin-binding epidermal growth factor-like growth factor and basic fibroblast growth factor: a potential pathologic role. *Proc. Natl. Acad. Sci. USA*, **92**: 6547–6551, 1995.
- Kume, N., and Gimbrone, M. J. Lysophosphatidylcholine transcriptionally induces growth factor gene expression in cultured human endothelial cells. *J. Clin. Invest.*, **93**: 907–911, 1994.
- Dluz, S. M., Higashiyama, S., Damm, D., Abraham, J. A., and Klagsbrun, M. Heparin-binding epidermal growth factor-like growth factor expression in cultured fetal human vascular smooth muscle cells. Induction of mRNA levels and secretion of active mitogen. *J. Biol. Chem.*, **268**: 18330–18334, 1993.

45. Wyckoff, J. B., Insel, L., Khazaie, K., Lichtner, R. B., Condeelis, J. S., and Segall, J. E. Suppression of ruffling by EGF in chemotactic cells. *Exp. Cell Res.*, *242*: 100-109, 1998.
46. Kaufmann, A. M., Khazaie, K., Wiedemuth, M., Rohde-Schulz, B., Ullrich, A., Schirmacher, V., and Lichtner, R. B. Expression of epidermal growth factor receptor correlates with metastatic potential of 13762NF rat mammary adenocarcinoma cells. *Int. J. Oncol.*, *4*: 1149-1155, 1994.
47. Lichtner, R. B., Kaufmann, A. M., Kittmann, A., Rohde-Schulz, B., Walter, J., Williams, L., Ullrich, A., Schirmacher, V., and Khazaie, K. Ligand mediated activation of ectopic EGF receptor promotes matrix protein adhesion and lung colonization of rat mammary adenocarcinoma cells. *Oncogene*, *10*: 1823-1832, 1995.
48. Kaufmann, A. M., Lichtner, R. B., Schirmacher, V., and Khazaie, K. Induction of apoptosis by EGF receptor in rat mammary adenocarcinoma cells coincides with enhanced spontaneous tumour metastasis. *Oncogene*, *13*: 2349-2358, 1996.
49. Morris, V. L., MacDonald, I. C., Koop, S., Schmidt, E. E., Chambers, A. F., and Groom, A. C. Early interactions of cancer cells with the microvasculature in mouse liver and muscle during hematogenous metastasis: videomicroscopic analysis. *Clin. Exp. Metastasis*, *11*: 377-390, 1993.
50. Ohtani, H. Stromal reaction in cancer tissue: pathophysiologic significance of the expression of matrix-degrading enzymes in relation to matrix turnover and immune/inflammatory reactions. *Pathol. Int.*, *48*: 1-9, 1998.
51. Dong, Z., Kumar, R., Yang, X., and Fidler, I. J. Macrophage-derived metalloelastase is responsible for the generation of angiostatin in Lewis lung carcinoma. *Cell*, *88*: 801-810, 1997.
52. Zeng, Z. S., and Guillem, J. G. Colocalisation of matrix metalloproteinase-9-mRNA and protein in human colorectal cancer stromal cells. *Br. J. Cancer*, *74*: 1161-1167, 1996.
53. Christensen, L., Wiborg, S. C., Heegaard, C. W., Moestrup, S. K., Andersen, J. A., and Andreassen, P. A. Immunohistochemical localization of urokinase-type plasminogen activator, type-1 plasminogen-activator inhibitor, urokinase receptor and $\alpha(2)$ -macroglobulin receptor in human breast carcinomas. *Int. J. Cancer*, *66*: 441-452, 1996.
54. Nielsen, B. S., Timshel, S., Kjeldsen, L., Sehested, M., Pyke, C., Borregaard, N., and Dano, K. 92 kDa type IV collagenase (MMP-9) is expressed in neutrophils and macrophages but not in malignant epithelial cells in human colon cancer. *Int. J. Cancer*, *65*: 57-62, 1996.
55. Edmonds, B. T., Wyckoff, J., Yeung, Y. G., Wang, Y., Stanley, E. R., Jones, J., Segall, J., and Condeelis, J. Elongation factor-1 α is an overexpressed actin binding protein in metastatic rat mammary adenocarcinoma. *J. Cell Sci.*, *109*: 2705-2714, 1996.

Imaging of Primary Tumors in Whole Animals Using Laser-based Tomography

John S. Condeelis, Joan G. Jones, Jeffrey B Wyckoff, and Jeffrey E. Segall

We have developed a model in which the motility, adhesion and cell-cell interactions can be examined in live primary tumors in whole animals. Subcutaneous injection of GFP-expressing cells with graded metastatic potential into the mammary fat pad of female Fischer 344 rats generates primary tumors that fluoresce when GFP excited. Moving cells are imaged in the live rats under anesthesia, with either a laser scanning confocal or a multiphoton microscope. Imaging at high resolution in the non-metastatic and metastatic tumors demonstrates significant differences between the two which account for differences in metastatic potential (see abstract by Segall et al.). Non-metastatic tumors are more fibrous and less necrotic with tumor cells that are highly polarized and less motile. Metastatic tumors are more necrotic with tumor cells that are unpolarized except near blood vessels where they are highly polarized with cell protrusions toward the vessel. Metastatic cells move in groups or streams of cells suggesting a preferred micro-environment for locomotion and probable chemotaxis *in vivo*. Comparison of imaging with the laser scanning confocal and multiphoton microscopes demonstrates the greater imaging depth of the multiphoton microscope (~10x) in these breast tumors. This allows direct and rapid observations of the blood vessel distribution in primary tumors. Multiphoton imaging also permits visualization of extracellular matrix directly due to its autofluorescence in the near UV allowing the observation of cell adhesion and proteolysis *in vivo* and its correlation with cell motility. This is the first model that allows direct observations of metastasis in an intact orthotopically grown primary tumor while in the live animal.

The Rate-limiting Step in Metastasis: *In vivo* Analysis of Intravasation at the Primary Tumor Jeffrey E. Segall, Jeffrey B Wyckoff, Maryse Bailly, Joan G. Jones, and John S. Condeelis

Determination of the rate-limiting step in tumor cell metastasis is critical for evaluating the cell mechanisms controlling metastasis. Using GFP transfectants of the metastatic MTLn3 and non-metastatic MTC cell lines derived from the rat mammary adenocarcinoma 13762 NF, we have measured tumor cell density in the blood, individual cells in the lungs, and lung metastasis. Correlation of blood burden with lung metastases indicates that entry into the circulation is a rate-limiting step for metastasis for both metastatic and non-metastatic cell lines. Consistent with previous work, cell arrest in the lungs is efficient, while growth of metastases in the lungs is inefficient. To examine cell behavior at the critical step of intravasation, we have used GFP technology to view these cells in time lapse images within a single optical section using a confocal microscope (see abstract by Condeelis et al.). *In vivo* imaging of the primary tumors of MTLn3 and MTC cells indicates that both metastatic and non-metastatic cells are motile and show protrusive activity. However, metastatic cells show greater orientation towards blood vessels, and larger numbers of host cells within the primary tumor, while non-metastatic cells show greater fragmentation. Metastatic cells show chemotactic responses to EGF *in vitro*, and such responses *in vivo* may enable metastatic cells to avoid fragmentation and thus enhance their ability to survive entry into the circulation. These results demonstrate that cell-based assays for determination of cell properties *in vivo* are necessary for dissection of the metastatic process.